Ligand-Centered Oxidation in a Diiron *s*-Indacene Complex

Paul Roussel,† Douglas R. Cary,† Stephen Barlow,† Jennifer C. Green,† François Varret,‡ and Dermot O'Hare*,†

Inorganic Chemistry Laboratory, South Parks Road, Oxford, U.K. OX1 3QR, and Laboratoire LMOV, Université de Versailles, 45 Avenue des États-Unis, 78035 Versailles Cedex, France

Received November 29, 1999

The reaction of 1,3,5,7 tetra-*tert*-butyl-*s*-indacene (Ic′) with $[Fe_2(CO)_9]$ gives the bimetallic complex $[\{Fe(CO)_3\}_2Ic']$, **1**, where the two $Fe(CO)_3$ fragments are coordinated to the same face of the Ic′ ligand. The cyclic voltammogram of **1** displays two quasi-reversible molecular oxidation waves and an irreversible molecular reduction wave. **1** can be chemically oxidized to its monocation with silver tetrafluoroborate. Comparison of the crystal structures of **1** and $[\{Fe(CO)_3\}_2Ic']^+[BF_4]^-\cdot CH_2Cl_2$, **2**, shows little change in bond lengths on oxidation. Although, at first glance, **2** may appear to be an Fe^0/Fe^I mixed-valence compound, Mössbauer and EPR spectroscopy suggest that that the ionized electron originates from a largely indacene-based orbital. The structural and spectroscopic features of **1** and **2** have been rationalized by density functional calculations and compared to those of related systems.

Introduction

Organometallic polymers potentially show a range of interesting electronic and magnetic properties, some of which arise from intermetallic communication.[1] Studies of bimetallic model complexes indicate that the ligands *s*-indacene (Ic) and pentalene (Pn) are particularly effective at promoting metal−metal interactions.[2] However, synthesis of transition metal pentalene oligomers has met with limited success owing to their poor solubility.[3] Therefore, we have been interested in using alkylated *s*-indacene ligands to synthesize transition metal oligomeric and model bimetallic complexes. However, we have found that 1,2,3,4,5,6,7,8-octamethyl-1,5-dihydro-*s*-indacene[4] (Ic^*H_2) could not be doubly deprotonated to the 14 π-electron aromatic dianion and that monomeric transition metal complexes incorporating this ligand were not significantly more soluble than unsubstituted indacene complexes.[5] We therefore turned to the Ic′ (Ic′ = 1,3,5,7-tetra-*tert*-butyl-*s*-indacene) ligand system.[6] Ic′ is a stable 12 π-electron anti-aromatic compound originally reported by Hafner and co-workers. In addition to polymers, we have been interested in bimetallic model complexes; we took advantage of the availability of neutral Ic′ to investigate new synthetic routes to indacene bimetallics. In the course of this work, we synthesized a diiron complex, **1**, from $[Fe_2(CO)_9]$. We have communicated the synthesis and crystal structure of **1**;[7] here we report more fully on this compound and its one-electron oxidation product, **2**. We also compare the electronic structure of **1** and **2** with those of other organometallic derivatives of fused-ring ligands.

Experimental Section

General Experimental Details. All manipulations were carried under an inert atmosphere of argon or dinitrogen either using standard Schlenk lines or in a Vac Atmospheres drybox. NMR and EPR samples were made up in the drybox, and the sample tubes were sealed in vacuo or using Young's type concentric stopcocks. Solvents were distilled over potassium (tetrahydrofuran, toluene), sodium−potassium alloy (diethyl ether), and calcium hydride (dichloromethane, hexamethyldisiloxane) under an atmosphere of dinitrogen. NMR spectra were recorded on a Varian Unity 500 spectrometer and the spectra referenced internally, using the residual protio solvent resonances, to tetramethylsilane ($\delta = 0$ ppm). Infrared spectra were obtained in an airtight holder using a Perkin-Elmer FTIR spectrometer. Elemental analysis were performed by the analytical department, Inorganic Chemistry Laboratory, Oxford. Mass spectra were obtained from the EPSRC Mass Spectrometry Service, University of Wales, Swansea. Solid-state magnetic susceptibility data were measured on a Quantum design MPMS SQUID magnetometer using samples loaded in gelatin capsules; the data were corrected for sample diamagnetism by extrapolation of the high-temperature susceptibility data to infinite temperature. EPR spectra were recorded using an X-Band Varian spectrometer with an operating field of ca. 0.33 T and were referenced using 1,1-diphenyl-2-picrylhydrazyl ($g = 2.0037$). The Mössbauer measurements were obtained on microcrystalline samples using a constant-acceleration spectrometer with a 25 mCi ^{57}Co source. Isomer shift values are quoted relative to metallic iron at room temperature. Low temperatures were attained using an MD306 Oxford Instruments cryostat, controlled by an ITC4

† Inorganic Chemistry Laboratory.
‡ Laboratoire LMOV.

(1) Manners, I. *Adv. Organomet. Chem.* **1995**, *37*, 131−168.
(2) Barlow, S.; O'Hare, D. *Chem. Rev.* **1997**, *97*, 637−669.
(3) Oelckers, B.; Chávez, I.; Manríquez, J. M.; Román, E. *Organometallics* **1993**, *12*, 33.
(4) Barlow, S.; O'Hare, D. *Organometallics* **1996**, *15*, 3483−3485.
(5) Barlow, S.; Cary, D. R.; Drewitt, M. J.; O'Hare, D. *J. Chem. Soc., Dalton Trans.* **1997**, 3867−3878.
(6) Hafner, K.; Stowasser, B.; Krimmer, H. P.; Fischer, S.; Bohm, M. C.; Lindner, H. J. *Angew. Chem., Int. Ed. Engl.* **1986**, *25*, 630−632.
(7) Cary, D. R.; Webster, C. G.; Drewitt, M. J.; Barlow, S.; Green, J. C.; O'Hare, D. *Chem. Commun.* **1997**, 953−954.

10.1021/om990937c CCC: $19.00
Publication on Web 02/18/2000

Oxford Instruments temperature controller. The Mössbauer parameters were fitted using a least-squares procedure. Cyclic voltammograms were recorded using an EG&G potentiostat and software. The single-compartment airtight cell comprised a Pt disk working electrode, Pt wire auxiliary electrode, and Ag wire pseudo-reference electrode. Potentials were referenced to the ferrocenium/ferrocene couple by addition of ferrocene to the cell. [$AgBF_4$] was purchased from the Aldrich Chemical Co.; [$Fe(CO)_5$] and [$Fe_2(CO)_9$] were purchased from Strem Chemicals Inc.

Density functional (DF) calculations were carried out using the Amsterdam Density Functional package version 2.3.[8] Type IV basis sets used triple-ζ accuracy sets of Slater-type orbitals with a single polarization function added for main group elements (2p on H and 3d on C). The cores of the atoms were frozen: the C core up to the 1s orbital and Fe up to 2p. The generalized gradient approximation (GGA nonlocal) method was used, utilizing Vosko, Wilk, and Nusair's local exchange correlation,[9] with nonlocal exchange corrections by Becke[10] and nonlocal correlation corrections by Perdew.[11]

[{$Fe(CO)_3$}$_2$Ic′], 1. Toluene (30 cm^3) was added to a mixture of [$Fe_2(CO)_9$] (2.27 g, 6.24 mmol) and Ic′ [6] (1.95 g, 5.18 mmol); the mixture was then refluxed for 24 h. The resulting dark green solution was filtered and cooled to −30 °C to afford a dark green crystalline solid (2.24 g, 66%, 3 crops). Suitable crystals for X-ray diffraction were grown from slow cooling a concentrated solution of [{$Fe(CO)_3$}$_2$Ic′] in hexamethyldisiloxane. Anal. Calc for $C_{34}H_{40}O_6Fe_2$: C, 62.22; H, 6.14. Found: C, 61.79; H, 6.25. ^{1}H NMR (C_6D_6, 293 K): δ 5.39 (s, 2H, 2,6-Ic′); 5.23 (s, 2H, 4,8-Ic′); 1.19 (s, 36H, Bu^t). $^{13}C\{^1H\}$ NMR (C_6D_6, 293 K): δ 210.3 (s, CO); 98.1 (s, C-1, 3, 5, 7-Ic′); 88.6 (s, C-4, 8-Ic′); 87.2 (s, C-2, 6-Ic′); 37.0 (s, C-9, 10, 11, 12-Ic′); 32.5 (s, CMe_3); 30.8 (s, CMe_3). MS (FAB): *m*/*z* 656 (M^+), 628 (M^+ − CO), 572 (M^+ − 2{CO}), 544 (M^+ − 3{CO}), 516 (M^+ − 4{CO}), 488 (M^+ − 5{CO}). IR (CH_2Cl_2 soln): ν_{CO} 2036, 2001, 1972, 1942 cm^{-1}. IR (Nujol): ν_{CO} 2030, 1992, 1965, 1939 cm^{-1}.

[{$Fe(CO)_3$}$_2$Ic′]$^+$[BF_4]$^-$·CH_2Cl_2, 2. Tetrahydrofuran (20 cm^3) was added to a mixture of [{$Fe(CO)_3$}$_2$Ic′] (0.25 g, 0.38 mmol) and [$AgBF_4$] (0.075 g, 0.38 mmol); the mixture was stirred for 20 min. The solvent was sucked off under reduced pressure and the residue washed with diethyl ether (3 × 15 cm^3) and then extracted into dichloromethane (2 × 20 cm^3), filtered, and reduced in volume to ca. 10 cm^3 to give a dark green solution. Slow diffusion of diethyl ether (30 cm^3) into the solution afforded a dark green crystalline solid (0.234 g, 74%, 2 crops). Anal. Calc for $C_{35}H_{42}BO_6F_4Fe_2Cl_2$: C, 50.76; H, 5.11. Found: C, 51.22; H, 5.13. IR (CH_2Cl_2 soln): ν_{CO} 2081, 2055, 2028, 2004 cm^{-1}. IR (Nujol): ν_{CO} 2084, 2055, 2037, 1998 cm^{-1}.

Crystal Structure of 2. Single crystals of $C_{35}H_{42}BCl_2F_4Fe_2O_6$, fw = 832.12, were grown by slow cooling of a pentane solution. A green prism (0.6 × 0.3 × 0.3 mm^3) was mounted under paratone oil, cooled to 150 K on an Enraf-Nonius DIP-2000 image-plate diffractometer, and found to be monoclinic with a = 12.608(2) Å, b = 16.459(2) Å, c = 18.193(2) Å, β = 92.08(1)°, V = 3772(1) $Å^3$, Z = 4, and μ = 0.972 mm^{-1}. A total of 7891 independent {6955 with $I > 2\sigma(I)$} reflections were measured using Mo Kα radiation, with a step of 2° in the range 0−26.7° at 150 K. Frames were collected, indexed, and processed using DENZO,[12] and the files scaled together using SCALEPACK.[12] The structure was solved in the space group $P2_1/n$ using SIR92[13] and refined using SHELXL-93;[14] all non-hydrogen atoms were revealed by the direct methods solution, while hydrogen atoms were placed in geometrically idealized positions and given isotropic thermal parameters according to the atoms to which they were connected. An absorption correction was applied using XABS2.[15] One of the *tert*-butyl groups (C23 and the attached methyl carbons) was clearly rotationally disordered; this was best modeled as one methyl carbon of unit occupancy and four of half-occupancy. Full refinement (457 parameters) on F^2 converged with final indices (all data) R = 0.071, R_w = 0.186, and S = 0.994, and with $\Delta\rho_{max}$ = 1.42 e $Å^{-3}$ and $\Delta\rho_{min}$ = −0.74 e $Å^{-3}$. All crystallographic calculations were performed using WingGX-98.[16]

Results and Discussion

Synthesis and Characterization of [{$Fe(CO)_3$}$_2$Ic′], 1. Our initial synthetic strategy for the preparation of transition metal bimetallic complexes incorporating the Ic′ ligand was salt elimination, utilizing the dianion of the ligand.[17] The unsubstituted *s*-indacene dianion has been used successfully in the synthesis of [$(SnMe_3)_2$Ic][18] and [$(MCp^*)_2$Ic] {M = Fe, Co, Ni},[19] while stepwise deprotonation and salt-elimination reactions were used to synthesize [$(RhCOD)_2$Ic] {COD is 1,5-cyclooctadiene}.[20] However, reaction of metal indacenide reagents of the type [$M_2(sol)_n$Ic′] (M = Li, K; sol = solvent) with a wide variety of transition metal complexes led to the isolation of Ic′ as the only identifiable product, suggesting that [Ic′]$^{2-}$ is highly reducing. Consistent with this hypothesis, cyclic voltammetry of THF solutions of Ic′ or [$M_2(sol)_n$Ic′] does not show any feature attributable to the [Ic′]$^-$/[Ic′]$^{2-}$ couple in the solvent window, and [Ic′]$^{2-}$ is only prepared under the most severe conditions.

However, we realized the availability of neutral 12 π-electron Ic′ offered the possibility of alternative synthetic routes to indacene bimetallics, possibly complementary to the 14 π-electron dianion route available for Ic. Hence we reacted Ic′ with a number of transition metal moieties known to react with dienes and found [$Fe_2(CO)_9$][7] and [$CoCp(C_2H_4)_2$] [21] reacted to give bimetallic species. Reaction of Ic′ with 1 equiv of [$Fe_2(CO)_9$] in refluxing toluene afforded a dark green solution of [{$Fe(CO)_3$}$_2$Ic′], **1**, as shown in Scheme 1. NMR spectroscopy showed only a single isomer to be present; X-ray structure determination[7] revealed this was the syn-isomer. Surprisingly, DF calculations (vide infra) do suggest the syn-isomer is slightly more stable than the anti; however, the energy difference is only 2 kJ mol^{-1}, which we do not consider as significant, thus suggesting little inherent thermodynamic reason for

(8) te Velde, G.; Baerends, E. J. *J. Comput Phys.* **1992**, *99*, 84−98.
(9) Vosko, S. H.; Wilk, L.; Nusair, M. *Can. J. Phys.* **1990**, *58*, 1200.
(10) Becke, A. D. *Phys. Rev.* **1988**, *A38*, 3098−3100.
(11) Perdew, J. P. *Phys. Rev.* **1986**, *B34*, 8822.
(12) Otwinowski, Z. *Data Collection and Processing, Proceedings of the CCP4 Study Weekend*; Otwinowski, Z., Ed.; Daresbury Laboratory: Warrington, U.K., 1993.
(13) Altomare, A.; Cascarano, G.; Giacovazzo, C.; Guagliardi, A.; Polidori, G.; Burla, M. C.; Camalli, M. *J. Appl. Crystallogr.* **1994**, *27*, 435.
(14) Sheldrick, G. M. *SHELXS93: A Program for Crystal Structure Refinement*; University of Göttingen: Germany, 1993.
(15) Parkin, S.; Moezzi, B.; Hope, H. *J. Appl. Crystallogr.* **1995**, *28*, 53−56.
(16) Farrugia, L. J. *WinGX: An integrated system of publically available windows programs for the solution, refinment, and analysis of single-crystal X-ray diffraction data*; University of Edinburgh: Scotland, 1998.
(17) Cary, D. R.; Green, J. C.; O'Hare, D. *Angew. Chem., Int. Ed. Engl.* **1997**, *36*, 2618−2620.
(18) Bell, W. L.; Curtis, C. J.; Eigenbrot, C. W.; Pierpont, C. G.; Robbins, J. L.; Smart, J. C. *Organometallics* **1987**, *6*, 266−273.
(19) Manriquez, J. M.; Ward, M. D.; Reiff, W. M.; Calabrese, J. C.; Jones, N. L.; Carroll, P. J.; Bunel, E. E.; Miller, J. S. *J. Am. Chem. Soc.* **1995**, *117*, 6182−6193.
(20) Bonifaci, C.; Ceccon, A.; Gambaro, A.; Manoli, F.; Mantovani, L.; Ganis, P.; Santi, S.; Venzo, A. *J. Organomet. Chem.* **1998**, *577*, 97−109.
(21) Roussel, P.; Drewitt, M. J.; Cary, D. R.; Webster, C. G.; O'Hare, D. *Chem. Commun.* **1998**, 2205−2206.

Scheme 1

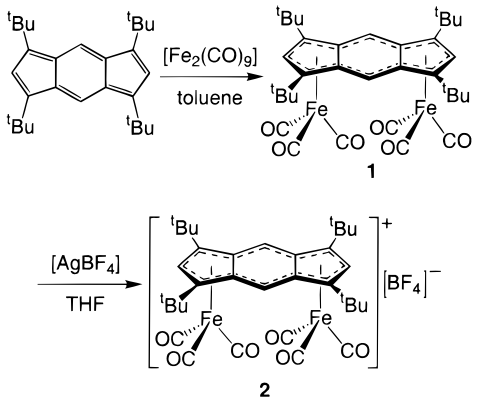

formation of the syn-isomer.[22] Since the dimeric nature of $[Fe_2(CO)_9]$ might be expected to favor formation of the syn-isomer, we wondered if use of monomeric $[Fe(CO)_5]$ would give an isomer mixture. Again we obtained only the syn-product. However, it is possible that the reaction proceeds via $[Fe_2(CO)_9]$ formed under the reaction conditions. $[(MCp^*)_2Ic]$ {M = Fe, Co, Ni}[19] and $[\{Mn(CO)_3\}_2Ic]$[18] have previously been obtained as exclusively anti-products (respectively using dilithium and bis(trimethyltin) derivatives of the ligand), while $[(RhCOD)_2Ic]$ [20] and $[(CoCp)_2Ic']$ [21] have been obtained as isomer mixtures (respectively using [(RhCOD)KIc] and neutral Ic′). Although the crystal structure of **1** shows the molecule to have approximate C_2 symmetry, the NMR data are consistent with a C_{2v} structure, presumably due to rapid interconversion between the two alternative C_2 structures.

The infrared spectrum of **1** shows four bands attributable to carbonyl stretches at 2036, 2001, 1972, and 1942 cm^{-1} (in dichloromethane solution). Four carbonyl stretches have also been reported for *syn*-[{Mn(CO)$_3$}$_2$-(2,7-dimethyl-*as*-indacene)];[23] the large number of bands in these compounds results from vibrational coupling between the two intermeshed $M(CO)_3$ groups. The stretching frequencies themselves are similar to those in $[Fe^0(diene)(CO)_3]$ complexes including η^4-cyclopentadiene complexes[24] and $[\{Fe(CO)_3\}_2(\mu\text{-}\eta^{:4}\eta^4\text{-fulvalene})]$.[25,26]

Redox Chemistry of [{Fe(CO)$_3$}$_2$Ic′]. The cyclic voltammogram of **1** in THF shows two quasi-reversible molecular oxidation waves at $E_{1/2} = -0.64$ V and +0.04 (−0.55 and +0.26 V in dichloromethane) and an irreversible wave at $E_{red} = -2.17$ V (vs ferrocenium/ferrocene).[27] We initially assumed the oxidation processes corresponded to successive oxidations of the metal centers.[7] However, we subsequently found that the neutral ligand in THF also shows two oxidation waves (albeit irreversible) at $E_{ox} = +0.10$ and +0.43 V (vs ferrocenium/ferrocene) and an irreversible reduction at $E_{red} = -3.10$ V. Values of $E_{1/2}$ (Ic′$^{\bullet+}$/Ic′) > +0.36 V and $E_{1/2}$ (Ic′/Ic′$^{\bullet-}$) = −1.45 V have been previously reported in dimethylformamide solution.[28,29]

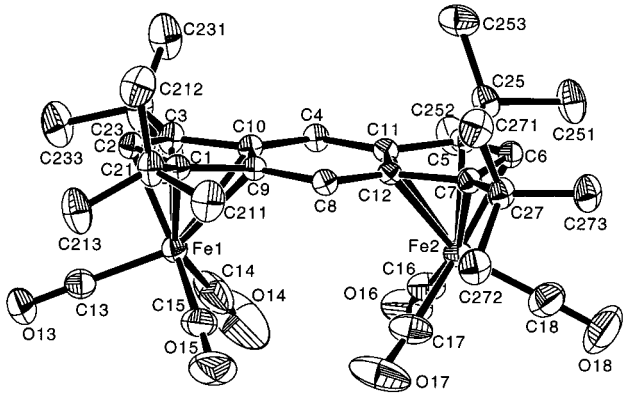

Figure 1. View of the cation in the crystal structure of $[\{Fe(CO)_3\}_2Ic']^+[BF_4]^-\cdot CH_2Cl_2$, **2** (50% thermal ellipsoids).

We attempted chemical oxidation of **1** to the mono- and dications. Although we were unable to synthesize the dication of **1** using a variety of reagents that, according to electrochemical data, should effect the oxidation, reaction of **1** with 1 equiv of silver tetrafluoroborate afforded a green paramagnetic crystalline solid, $[\{Fe(CO)_3\}_2Ic']^+[BF_4]^-\cdot CH_2Cl_2$, **2** (Scheme 1),[30] which we initially viewed as an Fe^0/Fe^I mixed-valence compound.

Crystal Structure of [{Fe(CO)$_3$}$_2$Ic′]$^+$[BF$_4$]$^-$·CH$_2$Cl$_2$, 2. Suitable crystals of **2** for single-crystal X-ray diffraction analysis were grown from a concentrated solution of dichloromethane and diethyl ether. The molecular structure is shown in Figure 1, while bond lengths are compared with those found for **1**[7] in Table 1 (an analogous atomic numbering scheme was used for **1**). In both structures the bimetallic molecule has approximate C_2 symmetry. In both structures the $Fe(CO)_3$ moieties are coordinated in a distorted η^5 fashion to the ligand; the bonds from iron to the ring-junction carbons are significantly longer than those to the other five-membered ring carbons. However, these distances (Fe1−9, Fe1−C10, Fe2−C11, Fe2−C12) are substantially diminished in **2** relative to **1**, as is the differences between Fe1−C9 and Fe1−C10 and between Fe2−C11 and Fe2−C12. The average Fe−CO bond length of 1.808(2) Å for **2** is marginally longer than that for **1** [1.788(7) Å]; concomitantly the C−O bond lengths in **2** [average 1.134(2) Å] are shorter than those found in **1** [average 1.156(3) Å]. The structures also differ in the rotational orientation of the $Fe(CO)_3$ moieties; this is presumably strongly dependent upon crystal-packing forces.

Spectroscopic Data for [{Fe(CO)$_3$}$_2$Ic′]$^+$[BF$_4$]$^-$·CH$_2$Cl$_2$, 2. The infrared spectrum of **2** has four stretches attributable to the carbonyl ligands at 2081, 2055, 2028,

(22) Optimisation of the geomtry of the model compound [{Fe(CO)$_3$}$_2$Ic], **I**, under C_{2h} (anti) and under C_{2v} and C_2 (syn) symmetry constraints gave energies of −244.59, −244.61, and −244.61 eV, respectively. No change in energy was found after relaxation of the symmetry constraints and further optimization. The optimized structure of *syn*-$[\{Fe(CO)_3\}_2Ic]^+$, **II**, gave an energy of −238.43 eV, leading to a prediction of 6.2 eV for the ionization energy of **I**.

(23) Bell, W. L.; Curtis, C. J.; Miedaner, A.; Eigenbrot, C. W.; Haltiwanger, R. C.; Pierpont, C. G.; Smart, J. C. *Organometallics* **1988**, *7*, 691−695.

(24) Zou, C.; Wrighton, M. S.; Blaha, J. P. *Organometallics* **1987**, *6*, 1452−1458.

(25) Delville, M.-H.; Lacoste, M.; Astruc, D. *J. Am. Chem. Soc.* **1992**, *114*, 8310−8311.

(26) Lacoste, M.; Delville-Desbois, M.-H.; Ardoin, N.; Astruc, D. *Organometallics* **1997**, *16*, 2343−2355.

(27) That is, $\Delta E_{1/2} = 0.68$ V in THF; 0.81 V in CH_2Cl_2. The first two oxidations of isoelectronic $[(CoCp^*)_2Ic]$ are also separated by 0.81 V in CH_2Cl_2.[19]

(28) Bachmann, R.; Gerson, F.; Geschiedt, G.; Hafner, K. *Magn. Reson. Chem.* **1995**, *33*, S60−S65.

(29) Using a correction of $E_{1/2}$(ferrocenium/ferrocene) = +0.45 V vs SCE in dimethylformamide (Connelly, N. G.; Geiger, W. E. *Chem. Rev.* **1996**, *96*, 877).

(30) **1** can also be oxidized using ferrocenium hexafluorophosphate.

Table 1. Bond Lengths (in Å) from the Crystal Structures of 1[7] and 2 Compared with Corresponding Calculated Distances in the Model Compounds I and II

	1	2	I	II
		Fe−Ic′ Bonds		
Fe1−C1	2.131(5)	2.114(3)	2.081	2.067
Fe1−C2	2.065(6)	2.076(3)	2.003	2.037
Fe1−C3	2.166(5)	2.133(4)	2.087	2.074
Fe1−C9	2.325(5)	2.251(3)	2.402	2.273
Fe1−C10	2.436(5)	2.305(3)	2.415	2.287
Fe2−C5	2.143(5)	2.120(3)	*a*	*a*
Fe2−C6	2.069(5)	2.086(4)	*a*	*a*
Fe2−C7	2.165(5)	2.125(3)	*a*	*a*
Fe2−C11	2.350(5)	2.262(3)	*a*	*a*
Fe2−C12	2.446(5)	2.296(3)	*a*	*a*
		Ic′ C−C Bonds		
C1−C2	1.420(7)	1.423(4)	1.420	1.416
C1−C9	1.452(6)	1.461(4)	1.440	1.442
C2−C3	1.420(7)	1.419(4)	1.420	1.416
C3−C10	1.467(6)	1.455(4)	1.440	1.441
C4−C10	1.384(6)	1.402(4)	1.387	1.391
C4−C11	1.416(7)	1.399(4)	*a*	*a*
C5−C6	1.418(6)	1.418(4)	*a*	*a*
C5−C11	1.449(6)	1.456(4)	*a*	*a*
C6−C7	1.428(6)	1.424(5)	*a*	*a*
C7−C12	1.456(7)	1.459(4)	*a*	*a*
C8−C9	1.413(6)	1.417(4)	1.389	1.393
C8−C12	1.383(6)	1.395(4)	*a*	*a*
C9−C10	1.459(6)	1.458(4)	1.447	1.451
C11−C12	1.462(6)	1.460(4)	*a*	*a*
		Fe−CO Bonds		
Fe1−C13	1.787(6)	1.811(4)	1.747	1.758
Fe1−C14	1.769(6)	1.804(5)	1.751	1.765
Fe1−C15	1.804(6)	1.821(5)	1.749	1.764
Fe2−C16	1.814(6)	1.806(4)	*a*	*a*
Fe2−C17	1.779(6)	1.814(4)	*a*	*a*
Fe2−C18	1.776(6)	1.798(5)	*a*	*a*
		C−O Bonds		
C13−O13	1.169(7)	1.132(5)	1.155	1.146
C14−O14	1.154(7)	1.118(6)	1.153	1.146
C15−O15	1.155(7)	1.138(6)	1.153	1.146
C16−O16	1.141(6)	1.130(5)	*a*	*a*
C17−O17	1.159(7)	1.130(5)	*a*	*a*
C18−O18	1.156(7)	1.142(6)	*a*	*a*
		Nonbonded Distances		
Fe1−Fe2	5.414(5)	5.048(3)	5.206	4.978
Fe1−C4	3.548(5)	3.415(3)	3.500	3.353
Fe1−C8	3.417(6)	3.399(3)	3.523	3.379
Fe2−C4	3.450(5)	3.415(4)	*a*	*a*
Fe2−C8	3.560(5)	3.346(3)	*a*	*a*

[a] Denotes redundant information due to the C_2 symmetry used in the calculations.

Table 2. Mössbauer Parameters for 1 and 2

	1		2	
temperature/K	δ/mm s^{-1}	Δ/mm s^{-1}	δ/mm s^{-1}	Δ/mm s^{-1}
4.2	0.182(1)	1.528(1)	0.182(1)	1.520(1)
77	0.173(1)	1.510(1)	0.173(1)	1.518(1)
295	0.087(1)	1.472(1)	0.101(1)	1.472(1)

and 2004 cm^{-1}. Thus, there is an average increase in stretching frequency of 56 cm^{-1} compared to **1**, indicative of less back-bonding from the Fe_2Ic' fragment, consistent with the increase in Fe−CO bond lengths and decrease in C−O bond lengths observed in the molecular structure (vide supra).

^{57}Fe Mössbauer spectra of **1** and **2** were recorded at various temperatures between 4.2 and 295 K (Table 2). Compound **1** displays a doublet resonance characterized by values of 0.173 mm s^{-1} and 1.51 mm s^{-1} for the isomer shift (δ) and quadrupole splitting (Δ) respectively at 77 K. These values are typical for [Fe^0(diene)(CO)$_3$] compounds.[31] Compound **2** exhibits a single doublet resonance, indicating that both iron centers are equivalent on the Mössbauer time scale. Moreover, the spectrum of **2** is essentially identical to that of **1**, suggesting that the oxidation state of the iron atoms is not affected by the oxidation, i.e., that the oxidation is ligand-based.

The room-temperature EPR spectrum of **2** in dichloromethane solution consists of a poorly resolved triplet centered at $g = 2.019$ with a proton hyperfine coupling constant (a_H) of ca. 0.3 mT. The EPR spectrum indicates that the unpaired electron couples strongly to only one of the pairs of equivalent protons on the Ic′ ligand. Using the McConnell equation, we can estimate that the unpaired electron spin density (ρ) on these C atoms is 0.13. The EPR spectrum is rather similar to the previously reported spectrum of [Ic′]$^{\bullet+}$ {generated in situ by oxidation with Tl(CF$_3$CO$_2$)$_3$ in CF$_3$CO$_2$H} which is a triplet characterized by $g = 2.003$ and $a_H = 0.22$ mT.[28,32] The large proton hyperfine coupling constant in **2** indicates the unpaired electron resides in an orbital with substantial ligand character, while the increased g value compared to that of [Ic′]$^{\bullet+}$ indicates some small degree of delocalization onto the metal centers. Solid-state samples of microcrystalline **2** show an anistropic powder pattern with $g_1 = 2.040$, $g_2 = 2.015$, and $g_3 = 1.994$ (6 K), again indicative of some delocalization onto the metal centers.[33] The solid-state magnetic susceptibility of **2** was measured in the temperature range 5−300 K. **2** exhibits Curie−Weiss paramagnetism in this temperature range ($C = 0.431$ emu K mol^{-1}, $\theta = -3.19$ K) and has a room-temperature magnetic moment of $\mu_{eff} = 1.84$ μ_B, close to the value of 1.74 μ_b expected for one unpaired electron and $\langle g \rangle = 2.016$.

Density Functional Calculations. To rationalize the bonding in **1** and the spectroscopic properties of **2**, we performed DF calculations on the simplified model compounds [{Fe(CO)$_3$}$_2$Ic], **I**, and [{Fe(CO)$_3$}$_2$Ic]$^+$, **II**. The geometries of **I** and **II** were optimized assuming C_2 symmetry; calculated bond lengths are compared with crystallographic values for **1** and **2** in Table 1. In general, the calculated values are in good agreement with the experimental data for both the neutral molecule and the cation. However, the asymmetry in Fe coordination, gauged by the difference between Fe1−C9 and Fe1−C10, and between Fe2−C11 and Fe2−C12, is underestimated for the neutral molecule. The chief changes in structure on oxidation (vide supra) are qualitatively reproduced, although the calculations somewhat underestimate the contraction in C−O bonds.

The energy level scheme in Figure 2 shows the π-orbitals of free Ic and their interaction with the two Fe(CO)$_3$ fragments in **I**. The π-orbitals for Ic closely resemble those previously obtained by extended Hückel methods,[28,34] although one such study found the orbitals equivalent to our π_6 and π_5 to be degenerate in unsubstituted Ic, but reversed in energy (relative to our scheme) on addition of *tert*-butyl substituents.[28] Our

(31) Herber, R. H.; King, R. B.; Wertheim, G. K. *Inorg. Chem.* **1964**, *3*, 101−107.
(32) Additional hyperfine coupling was also resolved in each component of the triplet.
(33) No hyperfine coupling was resolved in solid samples.
(34) Garland, M. T.; Saillard, J.-Y.; Chávez, I.; Oëleckers, B.; Manríquez, J.-M. *J. Mol. Struct.* **1997**, *390*, 199−208.

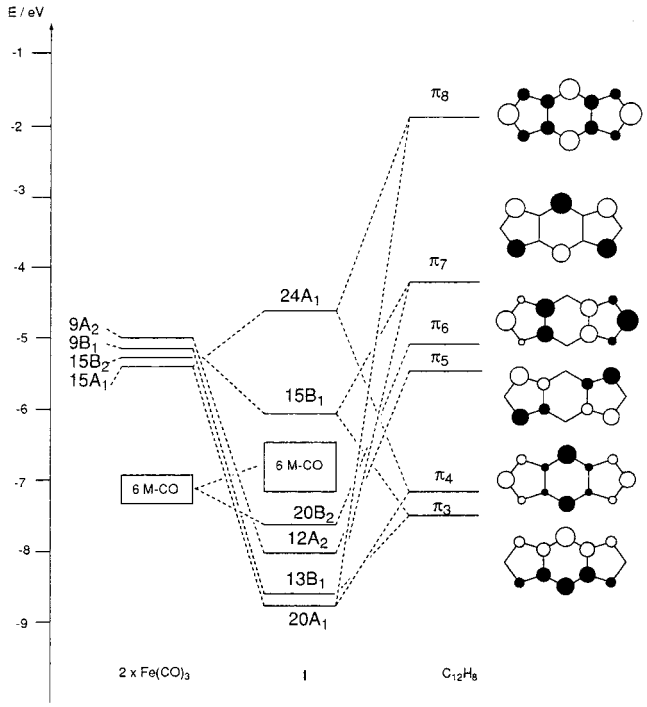

Figure 2. Molecular orbital scheme for [{Fe(CO)$_3$}$_2$Ic], **I**, according to DF calculations.

orbital scheme is consistent with the ESR spectrum reported for [Ic′]$^{\bullet+}$; the unpaired electron resides in an orbital resembling π_6 and, therefore, couples strongly to the two protons on the five-membered rings (those in the 2- and 6-positions).

The interaction between the Fe(CO)$_3$ fragments and the five-membered rings of the ligand closely resembles that between an M(CO)$_3$ fragment and a cyclopentadienyl ring. This interaction is expressed in the set of 10 orbitals lying between −8.6 and −6.3 eV in energy, the six higher energy orbitals being primarily Fe−CO back-bonding in character and the four lower orbitals representing the main metal−indacene interaction. Mixing of π_7 with π_3 and π_4 with π_s maximizes the Fe−Ic interaction by increasing the electron density on the five-membered rings below which the iron atoms lie. Consequently the HOMO (24A$_1$) and HOMO-1 (15B$_1$) also comprise mixtures of π_3 and π_7, and of π_4 and π_8, respectively; these two orbitals are shown in Figure 3. The corresponding orbitals of **II** (where 24A$_1$ is the SOMO) are very similar. The ligand contributions to these two orbitals are primarily from the two CH carbons of the six-membered ring, but there is also some metal contribution. To obey the 18-electron rule, a transition metal dimer lacking a metal−metal bond is expected to have 36 valence electrons. If the Ic′ ligand is regarded as a 12-electron ligand, then **1** and **I** are 40-electron complexes. It is the two orbitals shown in Figure 3 that accommodate the four excess electrons. In the case of the HOMO, the metal−ligand interaction is somewhat antibonding between the Fe(CO)$_3$ moieties and the ligand. This explains the observed decrease in the metal−ring junction carbon bond lengths on oxidation and the concomitant decreases in Fe−C4, Fe−C8, and Fe1−Fe2.

The calculations suggest a spin density of 0.32 on each Fe of **II** and 0.16 on C4 and on C8. The calculated spin

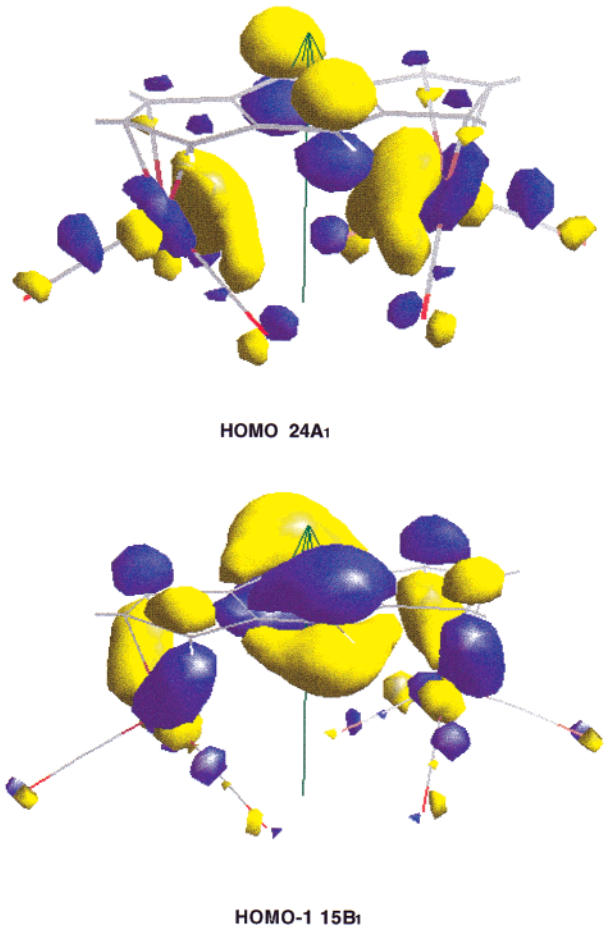

Figure 3. Representations of the HOMO and HOMO-1 of [{Fe(CO)$_3$}$_2$Ic], **I**, according to DF calculations.

densities on C4 and C8 are in excellent agreement with the value estimated from the EPR data (vide supra). Therefore, we conclude that the triplet coupling observed in the solution EPR spectrum must arise from strong coupling to the two equivalent six-membered ring protons (attached to C4 and C8); this is in contrast to the spectrum of [Ic]$^{\bullet+}$, where a superficially similar triplet arises from coupling to the two *five*-membered ring protons (attached to C2 and C6). The magnitude and anisotropy of the **g** tensor of **2** are explained by the iron contributions to the SOMO of **II**. However, Mössbauer results perhaps suggest a greater degree of ligand localization for the oxidation than the calculations.

Discussion. The most obvious compounds with which to compare **1** and **2** are the variety of fused-ring bimetallics [(MCp*)$_2$L] {M = Fe, Co, Ni; L = Pn, Ic, *as*-indacene} studied by Manriquez and co-workers.[19,34−37] Mössbauer spectra for their diiron compounds all show substantial changes on one-electron oxidation, suggesting more metal-based HOMOs than that of **1**;[19,36−38] the changes parallel those for typical ferrocene/ferrocenium

(35) Bunel, E. E.; Valle, L.; Jones, N. L.; Carroll, P. J.; Barra, C.; Gonzalez, M.; Munoz, N.; Visconti, G.; Aizman, A.; Manriquez, J. M. *J. Am. Chem. Soc.* **1988**, *110*, 6596.

(36) Reiff, W. M.; Manriquez, J. M.; Ward, M. D.; Miller, J. S. *Mol. Cryst. Liq. Cryst.* **1989**, *176*, 423−428.

(37) Reiff, W. M.; Manriquez, J. M.; Miller, J. S. *Hyperfine Interact.* **1990**, *53*, 397−402.

(38) [(FeCp*)$_2$Pn] (34e) and [(FeCp*)$_2$Ic] (38e) both give Mössbauer-delocalized cations on oxidation, whereas [(FeCp*)$_2$(*as*-indacene)] (38e) gives a more localized cation (indicating a class II Fe^{II}/Fe^{III} mixed-valence compound).

systems. Moreover, comparison of the crystal structures of $[(FeCp^*)_2Ic]$ and $[(FeCp^*)_2Ic]^+[BF_4]^-$ [19] shows a shortening of Fe−C bond lengths, indicating the HOMO/SOMO to be substantially antibonding (consistent with extended Hückel calculations for the unmethylated analogue[34]). Bond lengthening is seen on oxidation of the pentalene complex,[19,35] again consistent with calculations.[34]

A better comparison is perhaps $[(CoCp^*)_2Ic]$, since it is isoelectronic with **2**. Extended Hückel calculations predict a HOMO for $[(FeCp)_2Ic]^{2-}$ (also isoelectronic with **1**) resembling that of **1** insofar as the main ligand component is localized on the two CH carbons of the six-membered ring.[34] Unfortunately, the published calculations do not indicate the overall appearance of this orbital. Nevertheless, there is also a marked similarity in the electrochemistry of **1** and $[(CoCp^*)_2Ic]$.[19,27] Obviously, Mössbauer data for $[(CoCp^*)_2Ic]$ are not available, and unfortunately, neither neutral nor monocationic species is structurally characterized. $[(NiCp^*)_2Ic]^{2+}$, although also isoelectronic with **1**, appears to have two unpaired electrons,[19] despite the prediction of a large HOMO−LUMO gap for $[(FeCp)_2Ic]^{2-}$.[34] Unsurprisingly, replacement of the bridging ligand of $[(CoCp^*)_2Ic]$ with *as*-indacene leads to significantly different properties, owing to differences in electronic structure of the two ligands.

It is also interesting to compare the electronic structure of **1** with those of the $[Pn''_2M_n]$ {Pn″ = 1,4-bis(triisopropylsilyl)pentalene); M_n = Mo_2, Th, U} sandwich compounds recently reported by Cloke and coworkers.[39−41] DF calculations (on the unsilylated analogue) and UV−PES show the dimolybdenum species to have a mainly metal-based HOMO that is Mo−Mo antibonding and Mo−C bonding in character.[42] However, the HOMO of $[Pn''_2Th]$ is 83.7% ligand-based (although with considerable Th−Pn bonding character), suggesting ionization of this molecule could be considered as a ligand-based oxidation.[41] We also note briefly a rather different example of a ligand-based oxidation; bis(ruthenocenyl)ethylene undergoes a two-electron oxidation, accompanied by structural rearrangement, to $[(CpRu^{II})_2(\mu\text{-}\eta{:}^6\eta^6\text{-pentafulvadiene})]^{2+}$.[43,44] Thus, there is a continuum between more or less fully metal-based oxidations and those that are fully ligand-based. **1** and the isoelectronic $[(CoCp^*)_2Ic]$ mentioned above occupy an unusual position because, although the HOMOs have both ligand and metal character, the HOMOs are neither significantly bonding nor antibonding between the metal and the directly ligated atoms. The rather modest structural changes obtained on oxidation of **1** are due to interactions between the iron and the nonbonded CH carbons of the six-membered ring.

Conclusions

In conclusion, the oxidation of $[\{Fe(CO)_3\}_2Ic']$ affords a cation, which, at first sight, appears to be the first example of an Fe^I/Fe^0 mixed-valence bimetallic. However, spectroscopic and theoretical studies show that there is substantial ligand character to the SOMO of this cation. We note that the incorporation of substantial ligand character into the HOMO of $[\{Fe(CO)_3\}_2Ic']$ means that the hole formed on oxidation is delocalized throughout the structure, thus suggesting that the goal of preparing metal−indacene polymers with interesting one-dimensional delocalization properties is indeed attainable.

Acknowledgment. We thank the EPSRC for financial support. Part of this work has been carried out using computational resources of a DEC 8400 multiprocessor cluster (Columbus/Magellan), provided by the U.K.Computational Chemistry Facility at Rutherford Appleton Laboratory (admin: Department of Chemistry, King's College London, Strand, London WC2R 2LS).

Supporting Information Available: Details of crystal structure determination for **2**. This material is available free of charge via the Internet at http://pubs.acs.org.

OM990937C

(39) Cloke, F. G. N.; Hitchcock, P. B. *J. Am. Chem. Soc.* **1997**, *119*, 7899−7900.
(40) Kuchta, M. C.; Cloke, F. G. N.; Hitchcock, P. B. *Organometallics* **1998**, *17*, 1934−1936.
(41) Cloke, F. G. N.; Green, J. C.; Jardine, C. N. *Organometallics* **1999**, *18*, 1080−1086.
(42) Cloke, F. G. N.; Green, J. C.; Jardine, C. N.; Kuchta, M. C. *Organometallics* **1999**, *18*, 1087−1090.
(43) Sato, M.; Kudo, A.; Kawata, Y.; Saitoh, H. *Chem. Commun.* **1996**, 25−26.
(44) Sato, M.; Kawata, Y.; Kudo, A.; Iwai, A.; Saitoh, H.; Ochiai, S. *J. Chem. Soc., Dalton Trans.* **1998**, 2215−2224.